



Palladium nanoparticles supported on 1,3-dicyclohexylguanidine functionalized Mesoporous silica SBA-15 as highly active and reusable catalyst for the Suzuki-Miyaura cross-coupling reaction

| | |
|-------------------------------|---|
| Journal: | <i>RSC Advances</i> |
| Manuscript ID: | RA-ART-11-2014-014668.R2 |
| Article Type: | Paper |
| Date Submitted by the Author: | 02-Feb-2015 |
| Complete List of Authors: | Veisi, Hojat; Payame Noor University, Aminimanesh, Abass; Payame Noor University(PNU),, Faraji, Ali Reza; Faculty of Chemistry, Pharmaceutical Sciences Branch, Islamic Azad University, Eivazi, Neda; PNU, |
| | |

Palladium nanoparticles supported on 1,3-dicyclohexylguanidine functionalized Mesoporous silica SBA-15 as highly active and reusable catalyst for the Suzuki-Miyaura cross-coupling reaction

Hojat Veisi,^{a,*} Abbas Amini Manesh,^a Neda Eivazi,^a Ali Reza Faraji^b

^aDepartment of Chemistry, Payame Noor University (PNU), 19395-4697 Tehran, Iran

^bYoung Researchers & Elite Club, Pharmaceutical Sciences Branch, Islamic Azad University, Tehran, Iran

Fax +98(838)4227463; E-mail: hojatveisi@yahoo.com

Abstract. This paper described the simple procedure for synthesis and application of SBA-15/1,3-DCG/Pd as a novel nano catalyst in Suzuki-Miyaura cross-coupling reactions under atmospheric conditions in aqueous media. The SBA-15/1,3-DCG/Pd is air and moisture stable and readily prepared and the results indicated that palladium nanoparticles (Pd NPs) with an average size of 10 nm were uniformly dispersed onto inorganic support. Aryl halides, coupled with phenyl boronic acid smoothly afford the corresponding cross-coupling products with good to excellent yields (83-99 %). It was found that the catalytic system showed excellent activity for the Suzuki-Miyaura cross-coupling reaction of less reactive aryl chlorides with phenyl boronic acid. The reaction conditions have been evaluated considering the effect of various parameters such as reaction time, temperature, amount of catalyst, amount of base and its nature and solvent. The catalyst is completely recoverable with facile manner from the reaction mixture and the efficiency of the nano catalyst remains unaltered even after five cycles.

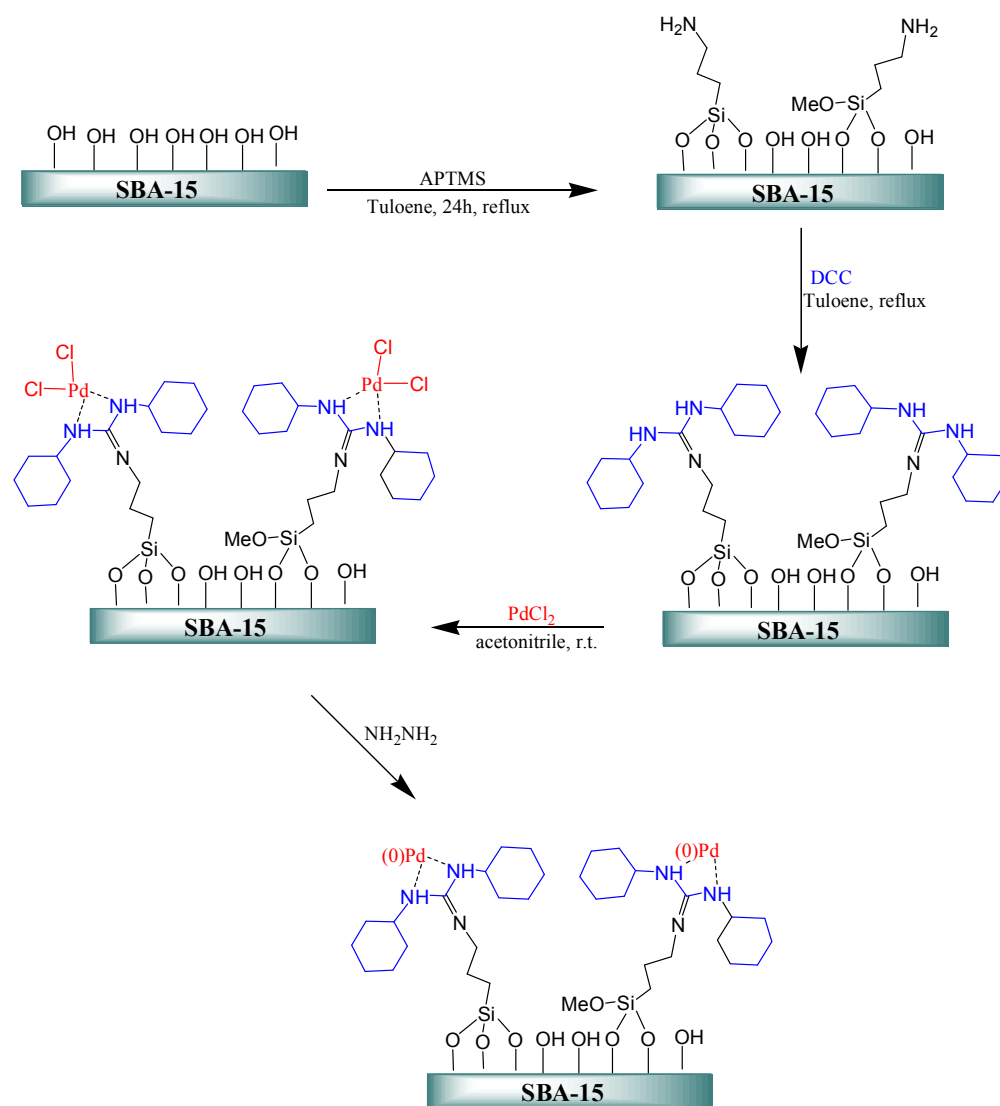
Keywords: Suzuki-Miyaura, Cross-coupling reaction, Palladium, Nano catalyst

Introduction

Today, the heterogenisation of metal complexes with catalytic activity within inorganic matrixes such as SiO₂,¹⁻³ MCM-41,^{4,5} SBA-15,⁶⁻¹¹ clay, zeolite and mesoporous materials is a field that has progressed due to the combination of high reactivity and chemical selectivity (like homogenous catalysts) with facile separation of the catalyst from the reaction mixture. Due to its properties, particular attention has been paid to reusability, thermal stability and low cost of the catalysts. In order to scientists and technologists have devoted much effort to the development of functionalized ordered Mesoporous silicas^{12,13} with high surface areas, tunable pore size and tailored composition has received great attention. These materials have broad application ranging gas separation,¹⁴ from adsorbent,¹⁵ and catalysis¹⁶⁻¹⁹ to biological uses.²⁰ Because of these materials have excellent properties such as mechanically stable structure, high surface area, and large, ordered pores with narrow size distribution of an inorganic backbone. This organic Mesoporous functionalization has been widely achieved by the grafting of functional groups. In particularly SBA-15 between other silica materials, Ordered mesoporous silicas (OMSs) have relatively high to good hydrothermal stability, and possesses hexagonal arrays of uniform pores with high special surface area and large pore volume.⁶⁻¹⁰

In past two decade, the use of palladium nanoparticles (Pd NPs) in catalysis has expanded considerably and has led to interesting applications both for fundamental research and industrial manufacturing.²¹ The catalytic formation of Carbon-Carbon bonds (such as the Suzuki, Heck, Sonogashira, Stille, Hiyama and Negishi reactions) is one of the most important reaction in organic synthesis. Among of these reactions, the Suzuki-Miyaura cross-coupling is one of the most important and useful transformations for the selective

construction of biaryls. This compound is applied in the synthesis of natural products, pharmaceuticals intermediates, optoelectronic devices, liquid crystal chemistry and advanced material.²²⁻²⁵ Due to the broad availability and low toxicity of its substrates (aryl boronic acids or borates and aryl halides or triflates) and its tolerance towards broad functional group and solvents, the SM cross-coupling reaction has found widespread applications in synthetic organic chemistry. Encouraged to our previous works on C-C-coupling reactions,²⁶⁻²⁸ in the present study, we designed and prepared SBA-15/1,3-DCG /Pd nanocatalyst (Scheme 1) by grafting of 1,3-dicyclohexylguanidine (1,3-DCG) groups on SBA-15 and subsequent deposition of Pd nanoparticles as a new and stable catalyst and investigated their performance in the Suzuki-Miyaura reactions for synthesis of biaryls (Scheme 2).



Scheme 1. Preparation of SBA-15/1,3-DCG /Pd.

Result and discussion

The formation of palladium catalyst onto the SBA-15 was verified using CHN analysis, UV-Vis, FT-IR, Size distribution (PSD), scanning electron microscope (SEM), transmission

electron microscope (TEM), Wavelength-dispersive X-ray spectroscopy (WDX), inductively coupled plasma (ICP-AES), energy-dispersive X-ray spectroscopy (EDX), X-ray diffraction (XRD) and X-ray photoelectron spectroscopy (XPS). The elemental analysis report along with summary of measured and calculated values for C, H and N is presented in Table 1. These data indicated the fact that the CHN content increased with the organic chain size because of immobilization of organic groups in the inorganic matrix.

By standard Brunauer–Emmett–Teller technique (BET) the specific surface area was analyzed. Nitrogen adsorption experiments were performed using 1 g of the nano catalyst. The surface area (S_{BET}), pore size (MPD) and volume (V_{BJH}) of the SBA-15, SBA-15-APTMS, SBA-15/1,3-DCG and SBA-15/1,3-DCG /Pd are listed in Table 1. The S_{BET} , V_{BJH} and MPD of the SBA-15/1,3-DCG were significantly reduced compared to the parent SBA-15 (this decrease indicates the decrease in interaction between adsorbate, N_2 molecules, and the nano-sized SBA-15 surface after modification with organic groups). Therefore this observation confirmed that the organic chain prefer to be grafted in the ordered nano pores. N_2 adsorption isotherms of SBA-15 and SBA-15/1,3-DCG /Pd are also shown in Fig. 1. The isotherms were all type IV with a H1 hysteresis loop and a steep increase in adsorption at relative pressures of 0.58–0.80 for SBA-15 samples approximately attributed to capillary nitrogen condensation according to IUPAC classification. This is typical for mesoporous materials with ordered pore structures.^{9,10} Additionally, upon modification the surface area and pore volume decreased obviously. These results are in good agreement with the fact that the surface modification indeed occurred inside the primary mesopores of the SBA-15.

The loading of palladium in the catalyst was determined by EDX and ICP analyses. The amount of Pd in nano catalyst was determined with an ICP-EAS instrument and final Pd content was measured around 0.30 mmol/g. This amount indicating that %75.6 of the immobilized ligands were complexed with palladium ions (see Table 1).

Table 1. Chemical composition and structural properties of the immobilized Pd-nano-catalyst on the SBA-15.

| Sample | Elemental analysis (wt%) ^a | | | Organic functional group (mmol/g) ^b | Immobilized –Pd Schiff base-complex (mmol/g) ^c | %Coordinate d Schiff base groups to Pd ions | Structural parameters ^d | | |
|--------------------|---------------------------------------|------|-----|--|---|---|--|---|----------------------|
| | C | N | Pd | | | | S_{BET} (m^2/g) | V_{BJH} (cm^3/g) | MPD (\AA) |
| SBA-15 | 0.46 | - | - | - | - | - | 782 | 0.99 | 59 |
| SBA-15-APTMS | 7.35 | 4.13 | - | 2.95 | - | - | 432 | 0.45 | 43 |
| SBA-15/1,3-DCG | 13.2 | 6.10 | - | 4.35 | - | - | 328 | 0.23 | 35 |
| SBA-15/1,3-DCG/Pd. | 11.3 | 2.10 | 1.3 | 1.50 | 0.30 | 75.6 | 285 | 0.18 | 27 |

^aNitrogen was estimated from the elemental analyses. Pd content determined from EDX analysis.

^b Determined from the N-contents.

^c Determined from the Pd-content, assume that palladium ions coordinated with 1.3-DCG ligands.

^d The pore size determined using the BJH method

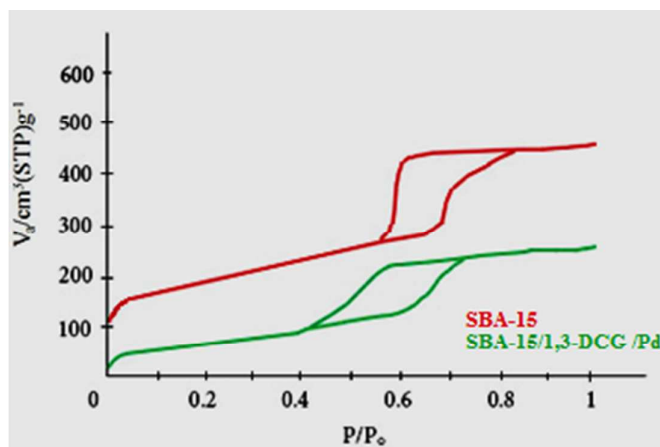


Fig 1. N₂-adsorption-desorption isotherms of SBA-15 and SBA-15/1,3-DCG/Pd.

The Pd loading of the prepared catalyst, measured by ICP, showed a value of about 0.30 mmol/g of catalyst. The elemental composition of the SBA-15/1,3-DCG/Pd samples was determined by EDX analysis. The result shown in Fig. 2 reveals that the nano catalyst contains Si, O, C and Pd.

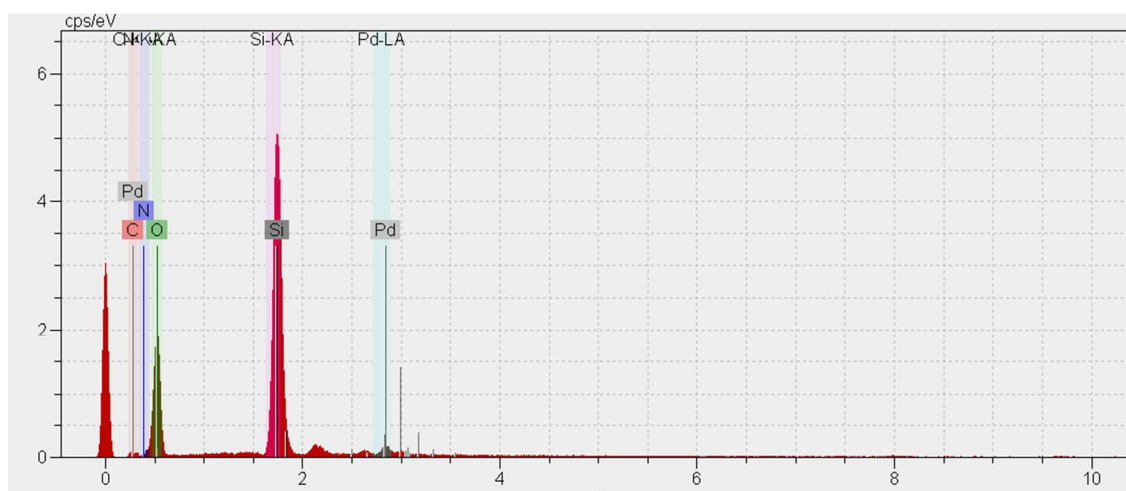


Fig 2. EDS spectrum of SBA-15/1,3-DCG/Pd.

FT-IR spectrum of SBA-15/1,3-DCG is shown in Fig. 2. In this section, the (ν), (σ), (s) and (as) represent stretching, bending, symmetric and asymmetric vibration, respectively. As it is seen in the spectrum of SBA-15,^{9,10} the structure is verified by the IR bands located at 3400 cm⁻¹ (ν_{as} O-H of silanols groups and adsorbed water), 1085 cm⁻¹ (ν_{as} Si-O), 807 cm⁻¹ (ν_s Si-O), 467 cm⁻¹ (σ Si-O-Si). C-H bending, vibration modes of the propyl in APTMS groups are observed between 1470 cm⁻¹ and 2850-2935 cm⁻¹.^{7,8} The N-H deformation peak at 1540–1561 cm⁻¹ indicates that the successful functionalization of the SBA-15 with trimethoxysilylpropylamine. Therefore, these results confirmed that the SBA-15 was successfully modified by amine spacer groups. The C=N imine vibrations signal was observed at 1650 cm⁻¹, which shows the condensation reaction between DCC with amino-functionalized SBA-15/pr-NH₂ (see Fig. 3).

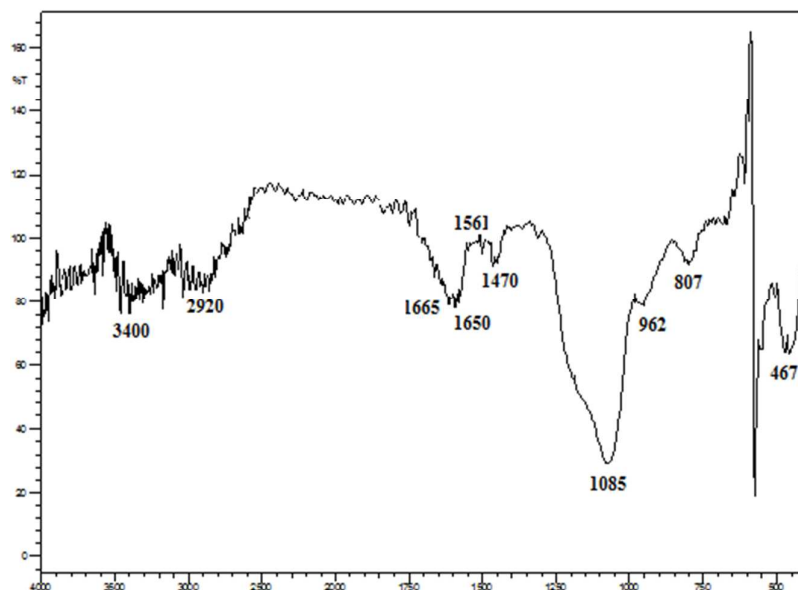


Fig. 3. FTIR spectra of SBA-15/1,3-DCG/Pd.

Typical SEM images with different magnifications for SBA-15/1,3-DCG/Pd are shown in Fig. 4. It reveals that the morphology of SBA-15/1,3-DCG/Pd consists of rod-shaped particles aggregated into bundles.

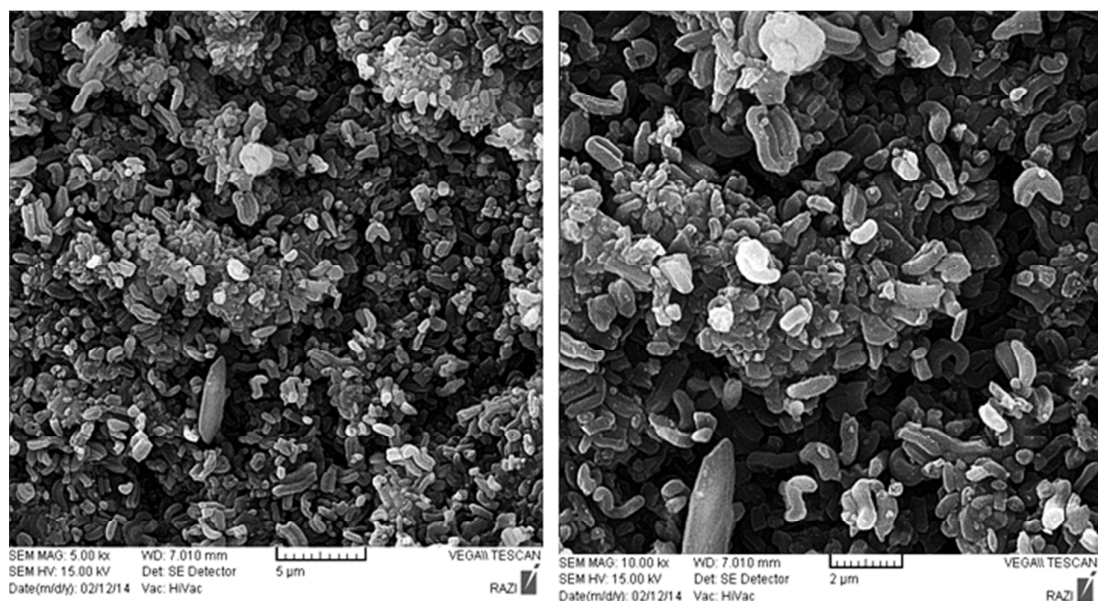


Fig. 4. SEM images of SBA-15/1,3-DCG/Pd.

The selected TEM images and its size distribution of the prepared catalyst are shown in Fig.5, from which it can be seen that the catalyst shows that the attachment of organic components to the SBA-15 materials has no distinct influence on the morphology of composition. It is seen that the average size Pd is in the range of 10 nm and palladium nanoparticles are dispersed on SBA-15. Particle Size Distribution Analysis (PSD) on

catalysts is a measurement designed to determine and report information about the size and range of a set of particles representative of a material. Therefore, PSD analysis of catalyst carried out. This analysis indicated that the average particle size in reverse microemulsion solution was around 10 nm (see Fig. 5b).

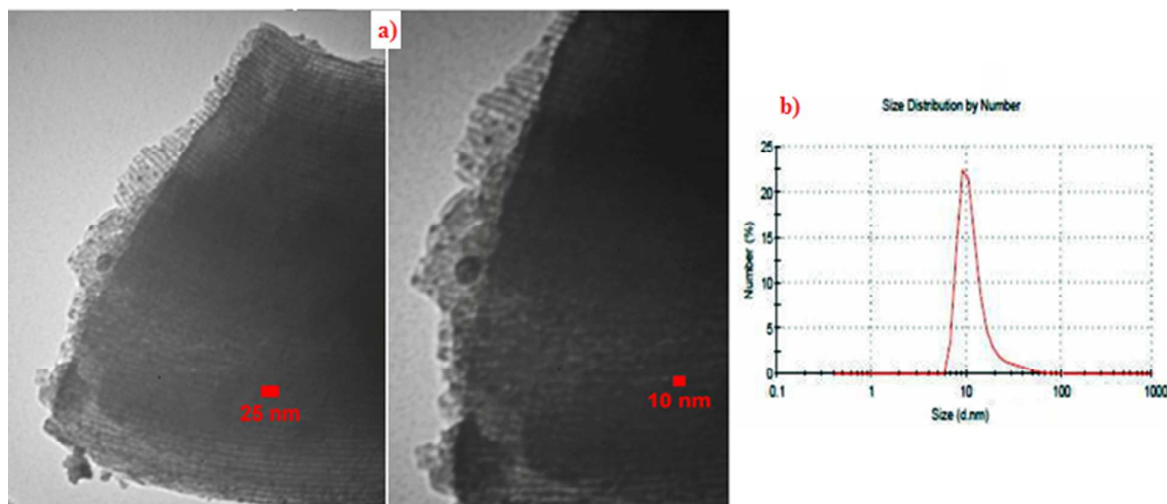


Fig. 5. (a) TEM images and (b) PSD Particle size distribution on the corresponding to SBA-15/1,3-DCG/Pd sample.

The low angle XRD patterns of SBA-15 and its functionalized derivatives and are shown in Fig. 6. Small angle X-ray powder diffraction of the parent SBA-15 gave the peaks in the 2θ range of 1–2.38 corresponding to 2D hexagonal $p6mm$ symmetry.^{29,9} The (1 1 0) and (2 0 0) reflections reveal long-range, mesopore ordering typical of SBA-15. After functionalization of SBA-15, the (1 0 0) and (2 0 0) reflections of the SBA-15 were remained but the intensity of peak was decreased. In addition, the (2 0 0) reflection was broadened and shifted marginally to higher 2θ values. The (1 1 0) reflection became weak and broad, which could be due to contrast matching between the silicate framework and organic moieties which are located inside the channels of SBA-15. These results indicated that the basic structure of the parent SBA-15 was not damaged in the whole process of catalyst preparation. These results agree well with those reported by others.^{9,10}

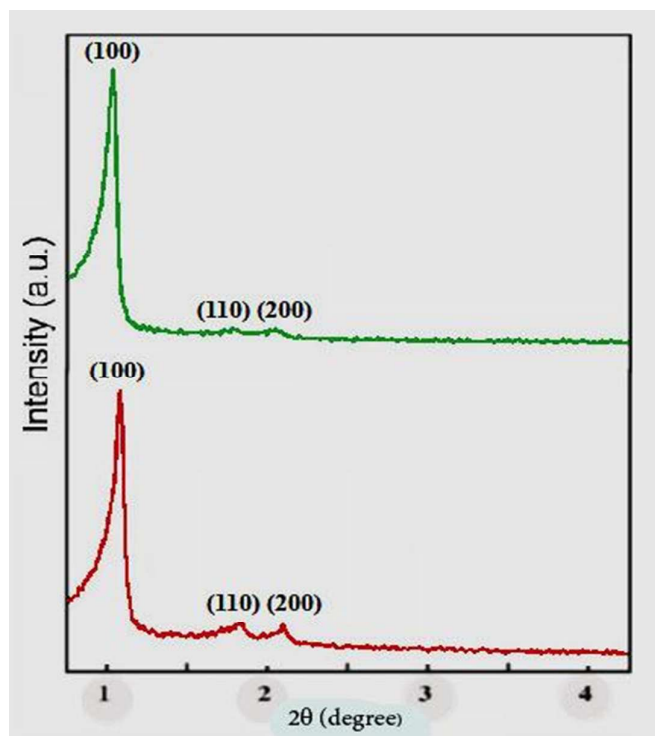


Fig. 6. XRD small angle patterns of the parent SBA-15 and SBA-15/1,3-DCG /Pd.

The X-ray diffraction (XRD) pattern in Fig. 7 shows the crystalline structure of the SBA-15/1,3-DCG /Pd catalyst. The XRD pattern of the SBA-15/1,3-DCG /Pd catalyst also shows Pd-NPs on the silica surface. The *f*-SBA-15-Pd nanocatalyst clearly exhibited (1 1 1), (2 0 0), (2 2 0) and (3 1 1) crystallographic planes of face-centered cubic (fcc) palladium at 39°, 46°, 67° and 82° respectively (JCPDS No. 89-4897).

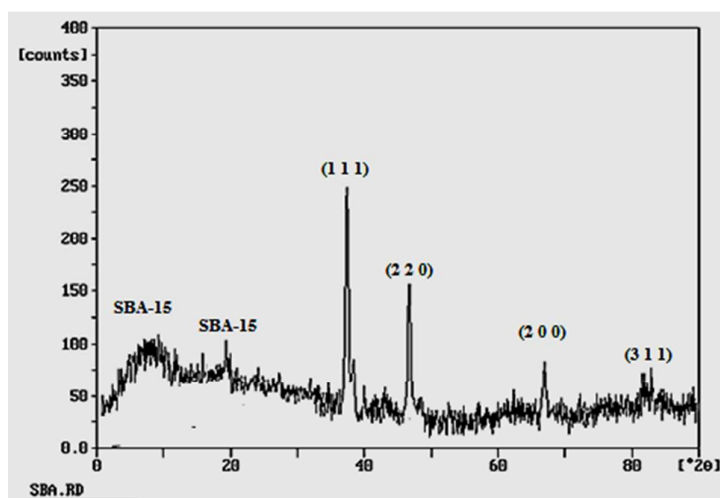


Fig. 7. XRD pattern of SBA-15/1,3-DCG/Pd.

The XPS spectroscopic analysis of the heterogeneous catalyst is a quantitative technique to indicate the electron properties of the species immobilized on the surface, such as oxidation state, the electron environment and the binding of the core electron (E binding) of the metal. Fig. 8 shows the XPS spectrum of SBA-15/1,3-DCG/Pd. The XPS spectrum of Si 2p contains a peak. This strong peak located at 104.3 eV, which is the typical Si 2p_{1/2}. Moreover, the study of the SBA-15/1,3-DCG/Pd at the Pd 3p level shows peaks at 531.7 and 554.2 eV for Pd 3p_{3/2}, which clearly indicates that the Pd nanoparticles are stable as metallic state in the nanocomposite structure. In comparison to the standard binding energy of Pd⁰, with Pd 3p_{3/2} of about 532.4 eV and Pd 3p_{1/2} of about 560.2 eV, it can be concluded that the Pd peaks in the SBA-15/1,3-DCG/Pd shifted to lower binding energy than Pd⁰ standard binding energy. The previous studies^{30,31} indicated that the position of Pd 3p peak is usually influenced by the local chemical/physical environment around Pd species besides the formal oxidation state, and shifts to lower binding energy when the charge density around it increases. Therefore, the peaks at 554.2 and 531.7 could be due to Pd⁰ species bound directly to 1,3-DCG in the SBA-15/1,3-DCG/Pd. The characteristic peaks corresponding to carbon (C 1s), nitrogen (N 1s) and oxygen (O 2s) are also clearly observed in XPS elemental survey of the SBA-15/1,3-DCG/Pd(0).

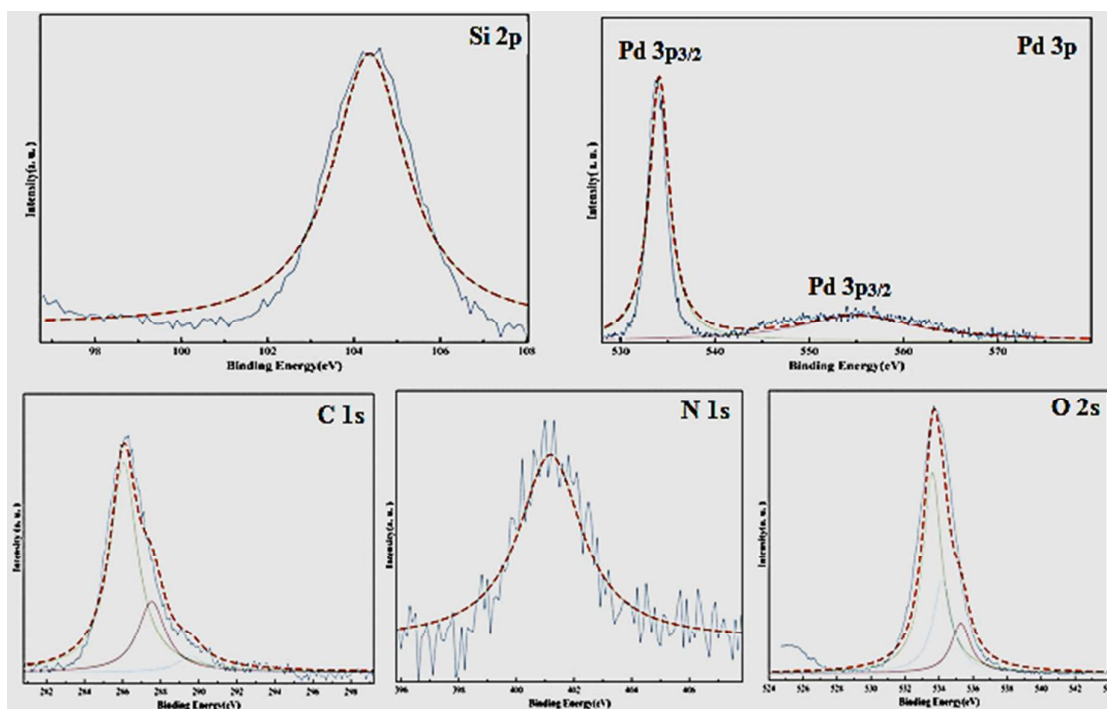


Fig 8. XPS image of the SBA-15/1,3-DCG /Pd.

In combination with scanning electron microscopy (SEM), wavelength-dispersive X-ray spectroscopy (WDX) can provide qualitative information about the distribution of different chemical elements in the catalyst matrix. Fig. 9 collects representative SEM and corresponding elemental maps (WDX) images for the synthesized catalyst. It can be seen that the particles are not fully spherical. In addition, some particle aggregations are observed, which is likely to be caused by the hydrogen interactions between particles. The WDX analysis reveals that Pd metal particles are well dispersed in the catalyst, which agrees well with the XRD and TEM analysis.

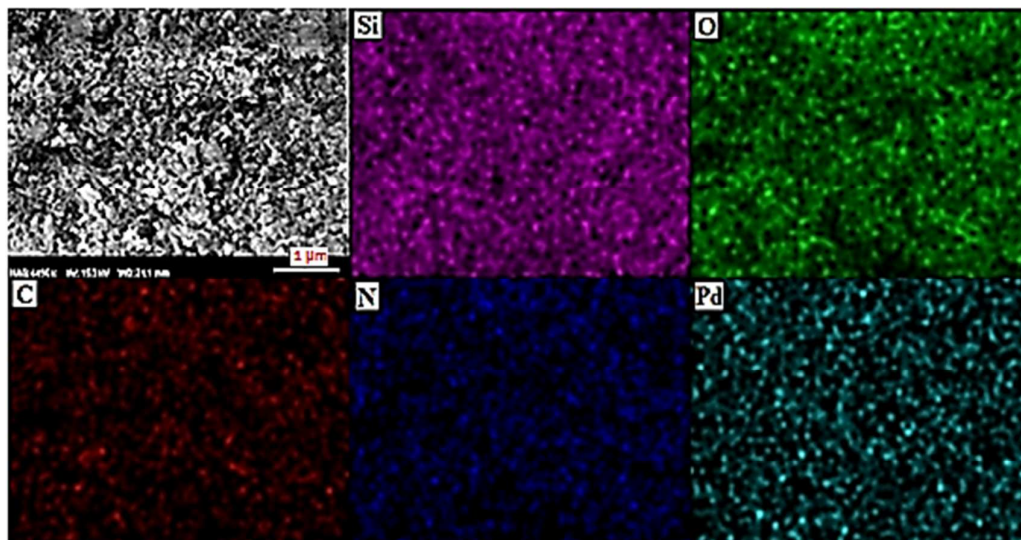
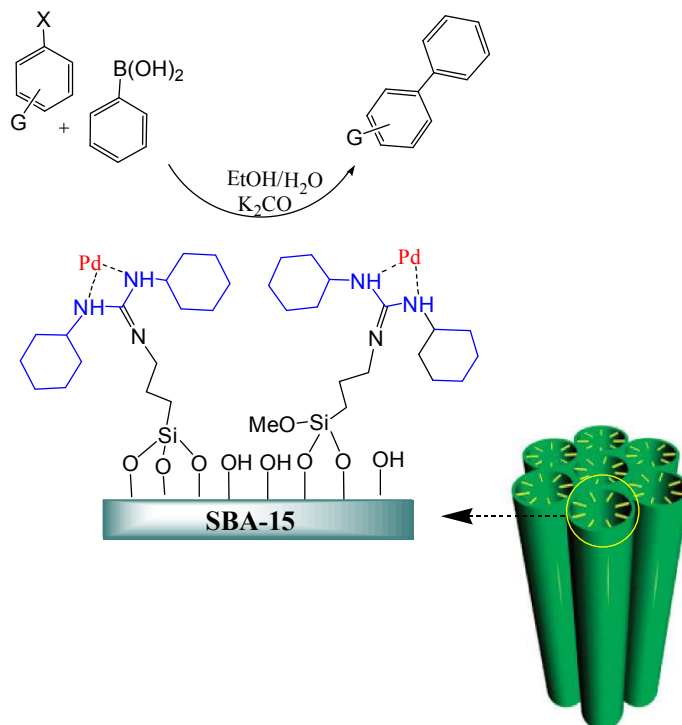


Fig. 9. SEM image of SBA-15/1,3-DCG/Pd and elemental maps of Si, O, C, N and Pd atoms of SBA-15/1,3-DCG/Pd.

After structure characterization of the prepared nanocatalysts (SBA-15/1,3-DCG/Pd), its catalytic activity was evaluated in the Suzuki reaction (Scheme 2).



Scheme 2. Suzuki-Miyaura reaction catalyzed by SBA-15/1,3-DCG/Pd.

The next investigation of this study was to optimize the conditions of the Suzuki coupling reaction by SBA-15/1,3-DCG/Pd. In our initial screens, more reaction parameters such as reaction temperature, solvent, type and amount base were investigated. The model substrate

for initial screening was phenyl iodide and phenylboronic acid leading to biaryl. Control experiments performed in the absence of the Pd NPs confirmed the crucial role of catalyst. The influence of the reaction temperature on the cross-coupling of phenyl iodide and phenylboronic acid catalyzed by SBA-15/1,3-DCG/Pd are summarized in Table 1. As shown in table 1, as the reaction temperature was increased to 60 °C, the yield of biaryl slightly increased. At room temperature biaryl could be synthesized in lower yield than 40 °C, although the mixture was stirred for prolonged reaction time (table1, entry 1). While the temperature rises to 40 °C the yield of biaryl increased rapidly (Table 1, entry 5).

Table 1. Effect of temperature.^a

| Entry | Nano catalyst (mg) | T (°C) | Time (h) | Yield (%) |
|-------|--------------------|--------|----------|-----------|
| 1 | 15 | 25 | 10 | 47 |
| 2 | 15 | 30 | 3 | 54 |
| 3 | - | 40 | 10 | trace |
| 4 | 5 | 40 | 3 | 78 |
| 5 | 10 | 40 | 0.5 | 99 |
| 6 | 5 | 50 | 3 | 81 |
| 7 | 10 | 50 | 0.5 | 99 |
| 8 | 10 | 60 | 0.5 | 99 |
| 9 | 10 | 70 | 0.5 | 99 |

^aReaction conditions: phenyl iodide (0.116 g, 1 mmol); phenyl boronic acid(0.134 g, 1.1 mmol) ; K₂CO₃ (0.276 mg, 2 mmol); water/ethanol (1:1), 4 cm³.

In order to show the effect of solvents upon the coupling reaction, the reaction of phenyl iodide reacted with phenylboronic acid in various solvent (nonpolar, protic and aprotic) in the presence of SBA-15/1,3-DCG/Pd at 40 °C. For this study many solvents such as DMF, 1,4-dioxane, EtOH, H₂O, THF, toluene and mixtures of two solvents (DMF/H₂O, DMF/EtOH and H₂O/EtOH) are considered. Using H₂O, EtOH, THF, or toluene did not favor the reaction, even on prolonging the reaction time to 5 h (Table 2, entries 1-6). But, when we adopted the H₂O/EtOH co-solvent, high yield of biaryl was obtained [8, 11]. The explanation may be attributed to the good solubility of the organic reactants and the inorganic base (Table 2, entries 10 and 11). The results indicated that the cross-coupling reaction proceeded in a higher yield (99 %) after 0.5 h. Therefore, H₂O/EtOH was recognized to be a more suitable reaction media for this coupling reaction.

Table 2. Effect of solvent and co-solvent.^a

| Entry | Solvent | Time (h) | Yield (%) |
|-------|----------------------------|----------|-----------|
| 1 | DMF | 5 | 13 |
| 2 | Toluene | 5 | 11 |
| 3 | THF | 5 | 14 |
| 4 | 1,4-dioxane | 5 | 8 |
| 5 | EtOH | 5 | 43 |
| 6 | H ₂ O | 5 | 46 |
| 7 | DMF/H ₂ O | 5 | 62 |
| 8 | DMF/EtOH | 5 | 39 |
| 9 | H ₂ O/EtOH(1:1) | 0.5 | 76 |
| 10 | H ₂ O/EtOH(1:1) | 0.5 | 78 |
| 11 | H ₂ O/EtOH(1:1) | 0.5 | 80 |
| 12 | H ₂ O/EtOH(1:2) | 0.5 | 99 |
| 13 | H ₂ O/EtOH(1:2) | 1 | 82 |

^aReaction conditions: Nano catalyst (10 mg); phenyl iodide (0.116 g, 1 mmol); phenyl boronic acid(0.134 g, 1.1 mmol); K₂CO₃ (0.276 mg, 2 mmol); T=40 °C.

The influence of the type and amount of different bases were also studied and the results are listed in Table 3. Various amounts of bases such as KOH, EtONa, *t*-BuONa, Na₂CO₃, K₂CO₃, Cs₂CO₃, NaOAc, NaOH and Et₃N were explored. It can be found that base and amount of it played a critical role in the cross-coupling system. The SM cross-coupling reaction stopped completely in the absence of K₂CO₃ (entry 1), indicating that the Pd NPs has excellent performance for activating Ar-Pd^{II}-X in the presence of K₂CO₃. It also seemed that the reaction rate was related closely with the amount of K₂CO₃. The higher molar ratio of K₂CO₃ could accelerate the cross-coupling reaction. The yield increased with the amount of K₂CO₃ rose from 1 to 2 mmol (entries 7 and 8), However, no significant difference was observed when the amount of K₂CO₃ was higher than 2 mmol (entry 9). In our optimization studies, results showed that the amount of K₂CO₃ was 2 eq to aryl halides (Table 3, entry 7).

Table 3. Effect of base.^a

| Entry | Base (base:Ph(OH) ₂ /mol:mol) | Time (h) | Yield (%) |
|-------|---|----------|--------------|
| 1 | - | 10 | - |
| 2 | EtONa (2:1) | 3 | 9 |
| 3 | <i>t</i> -BuONa (2:1) | 3 | 10 |
| 4 | Na ₂ CO ₃ (2:1) | 3 | 74 |
| 5 | NaOAc (2:1) | 3 | 11 |
| 6 | NaOH (3:1) | 3 | 10 |
| 7 | K ₂ CO ₃ (1:1) | 0.5 | 61 |
| 8 | K ₂ CO ₃ (2:1) | 0.5 | 99 |
| 9 | K ₂ CO ₃ (3:1) | 0.5 | 99 |
| 10 | K ₂ CO ₃ (1:1) | 3 | 64 |
| 11 | Et ₃ N (1:1) | 0.5 | 74 |
| 12 | Et ₃ N (2:1) | 0.5 | 76 |
| 13 | Et ₃ N (3:1) | 0.5 | 83 |

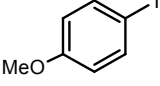
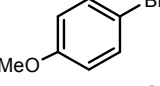
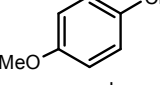
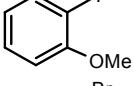
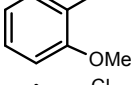
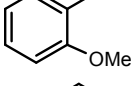
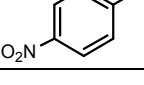
^aReaction conditions: Nano catalyst (10 mg); phenyl iodide (0.116 g, 1 mmol); phenyl boronic acid(0.134 g, 1.1 mmol); water/ethanol (1:1), 4 cm³; T=40 °C.

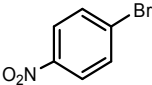
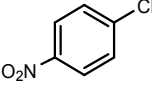
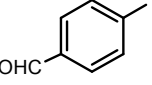
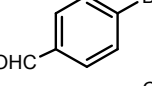
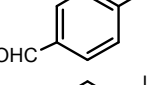
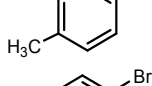
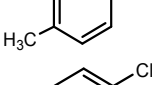
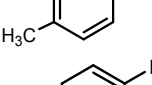
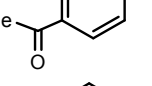
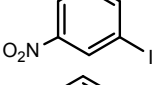
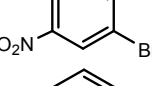
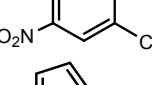
To widen the range of substrate, we examined the aryl iodides, bromides and chlorides with electron-withdrawing and electron-releasing groups and phenylboronic acid in the Suzuki-Miyaura reaction (Table 4). For characterize the products used the ¹H NMR, ¹³C NMR, FT-IR spectroscopy and elemental analysis. As shown in Table 4, high yields were obtained with both activated and non-activated aryl iodides (Table 4, entries 1, 4 and 10). Aryl iodides without any substituent and electron-deficient aryl halides are reactive substrates in Suzuki-Miyaura reactions and the related reactions went to completion in shorter reaction times. Next, the ability of Pd NPs to promote the SM cross-coupling for aryl chlorides and aryl boromides were studied. Indeed, the activation of aryl chlorides and aryl boromides by Pd NPs is a challenge for catalysis, in Suzuki-Miyaura reactions. Base on previous reports [22-25] for the aryl chlorides, harsher conditions are needed than those used for the activation of aryl bromides.

Further investigation showed that the relative reactivity of aryl halides in SBA-15/1,3-DCG/Pd catalyzed reactions is in the following order: R-I > R-Br > R-Cl. These results reflect the reactivity toward oxidative addition. Various substituents on aryl halides can

influence on the Suzuki-Miyaura cross-coupling reaction. Therefore, electron-withdrawing substituents on aryl halides increase the reaction rate and electron-donating substituents on aryl halides decrease the reaction rate. Suzuki-Miyaura cross-coupling reactions of aryl halide with electron-withdrawing groups (Table 4, entries 4-6) proceeded in shorter reaction times and gave coupled products in very good yields. By comparison of 4-bromobenzene and 2-bromobenzene indicated that an aryl bromide with an ortho substituent gave a lower yield than those with para or meta substituents which is presumably due to the absence of a steric effect from the 2-substituent (Table 4, entries 6 and 9). In the case of aryl chlorides with phenyl boronic acid, many of catalytic system did not efficiency precede the coupling even on harsh condition such as high temperature and extending the reaction time up to 24 h. In this investigation, we proved that the aryl chlorides with phenyl boronic acid were coupled without any limitation. The coupling reactions of aryl chlorides with phenyl boronic acid required longer times and gave moderate yields against with other aryl halide (Table 4, entries 3,12,15, and 18). In addition, 2-boromothiophene and 2-Iodomothiophene were coupled with phenyl boronic acid and gave the desired products with no poisoning of the palladium catalyst (Table 4, entry 23 and 24).

Table 4. Suzuki-Miyaura cross-coupling reaction of aryl halides with phenylboronic acid in aqueous media.

| Entry | Aryl halide | Time (h) | Yield (%) ^a |
|-------|---|----------|------------------------|
| 1 |  | 0.5 | 99 |
| 2 |  | 1.0 | 98 |
| 3 |  | 8 | 82 |
| 4 |  | 0.5 | 92 |
| 5 |  | 1.5 | 95 |
| 6 |  | 10 | 84 |
| 7 |  | 0.5 | 97 |
| 8 |  | 1.2 | 90 |
| 9 |  | 10 | 86 |
| 10 |  | 0.75 | 97 |

| | | | |
|----|---|-----|----|
| 11 |  | 2.5 | 93 |
| 12 |  | 12 | 80 |
| 13 |  | 1.2 | 97 |
| 14 |  | 3.5 | 91 |
| 15 |  | 6.0 | 83 |
| 16 |  | 0.5 | 96 |
| 17 |  | 2.0 | 94 |
| 18 |  | 10 | 85 |
| 19 |  | 2.0 | 94 |
| 20 |  | 0.5 | 99 |
| 21 |  | 1.2 | 94 |
| 22 |  | 12 | 82 |
| 23 |  | 1.2 | 94 |
| 24 |  | 2.2 | 90 |

^aReaction conditions: Nano catalyst (10 mg), Aryl halyde (1 mmol), phenylboronic acid (0.134 g, 1.1 mmol), K₂CO₃ (0.276 mg, 2 mmol), water/ethanol (1:1), 4 cm³, T=40 °C.

The reusability of the SBA-15/1,3-DCG/Pd was also checked (see Fig. 9). The cross-coupling reaction was carried out with phenyl iodide and phenyl boronic acid under the optimized reaction conditions. The nano-catalyst was separated from the reaction mixture by centrifugation and washed with water and chloroform. Then the solid catalyst was dried and reused for five times without significant loss in its catalytic activity.

In order to examine the leaching of Pd from the SBA-15/1,3-DCG/Pd as catalyst, we have used the hot filtration test. So, the reaction of phenyl iodide and phenyl boronic acid in the presence of SBA-15/1,3-DCG/Pd under optimized reaction condition was studied. In hot

filtration test, the solid catalyst was filtered off after 45% of the coupling reaction was completed and the liquid phase of the reaction mixture was kept in reaction condition for another 24 h. No increase in the amount of product was noticed. This result suggests that Pd is not being leached out from the solid catalyst during the cross-coupling reactions and the SBA-15/1,3-DCG/Pd behaved like a heterogeneous catalyst, which could be recovered and reused.

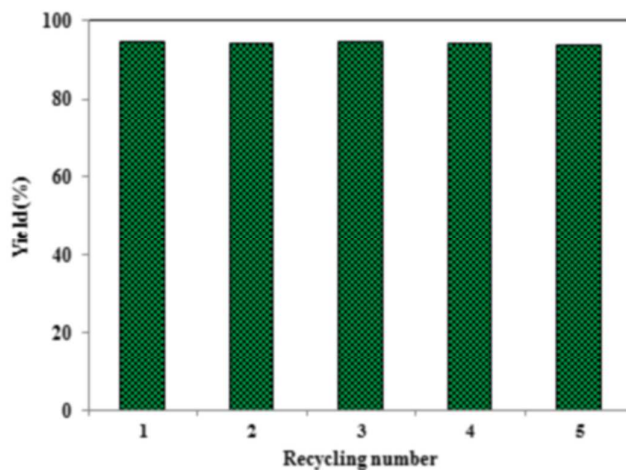


Fig. 9. Reusability of the nano catalyst in coupling reaction.

Conclusion

In this research, we have designed and synthesized a simple and efficient catalysis system of SBA-15 nano sized anchored palladium complexes with a number of bidentate ligands of *N, N* atoms in the Suzuki cross coupling reaction. This new heterogeneous catalyst showed the main advantages such as simple preparation, easy separation after reaction, mild condition reaction, high yield and selectively, widely used for different aryl halides and reusability for several times without any significant loss in its catalytic activity. Other extension of the method such as applying different catalysts is currently under investigation.

Experimental

Preparation of 1,3-dicyclohexylguanidine groups in SBA-15 (SBA-15/1,3-DCG)

To a 100 mL of round-bottom flask were introduced 30 mL of anhydrous toluene and 3.0 g of SBA-15 and 0.18 g (1.5 mmol) of 3-aminopropyl trimethoxysilane (APTMS) were added. The solution was refluxed for 24 h under an inert atmosphere, filtered and washed subsequently with toluene, dichloromethane, and methanol, and dried under reduced pressure at 80 °C for 24 h. In another 100 ml round-bottom flask, to a solution of 3 g of aminopropyl functionalized SBA-15 in 35 mL of toluene, 1 g of dicyclohexylcarbodiimide (DCC) was added and refluxed for 24 h. After completion of the reaction, the solid products were filtered and dried, and again washed with deionized water and then acetone and dried at 50 °C for 12 h (Scheme 1).

Immobilization of Pd(II) ions on the surface of SBA-15/1,3-DCG

2.0 g of SBA-15/1,3-DCG and 0.177 g of palladium chloride (1 mmol) in 50 mL of acetonitrile was stirred at room temperature for 4 h (Scheme 1). The brown resulting solid was filtered, washed with acetone and THF and dried in vacuum at 80 °C for 3 h to give SBA-15/1,3-DCG/Pd(II).

Reduction of Pd(II) ions on the surface of SBA-15/1,3-DCG

The reduction of SBA-15/1,3-DCG /Pd(II) by hydrazine hydrate was performed as follows: 50 mg of SBA-15/1,3-DCG /Pd(II) was dispersed in 60 mL of water, and then 100 μ L of hydrazine hydrate (80%) was added. The pH of the mixture was adjusted to 10 with 25% ammonium hydroxide and the reaction was carried out at 95 °C for 2 h. The final product SBA-15/1,3-DCG /Pd(0) was washed with water and acetone, and dried in vacuum at 50 °C.

Suzuki-Miyaura coupling reaction

In a typical reaction, 10 mg of the nano catalyst (10 mg = 0.003 mmol Pd) was placed in a 25 mL balloon, 1 mmol of the aryl halide in 4 mL of water/ethanol (1:2) was added 0.134 g (1.1 mmol) of phenyl boronic acid, 0.276 mg of K₂CO₃ (2 mmol). The mixture was then stirred for the desired time at 40 °C. The reaction was monitored by thin layer chromatography (TLC). After completion of reaction, the reaction mixture was cooled to room temperature and the catalyst was recovered by centrifuge and washed with ethyl acetate and ethanol. The combined organic layer was dried over anhydrous sodium sulfate and evaporated in a rotary evaporator under reduced pressure. The crude product was purified by column chromatography.

Acknowledgments. We are thankful to Payame Noor University (PNU) for partial support of this work.

References

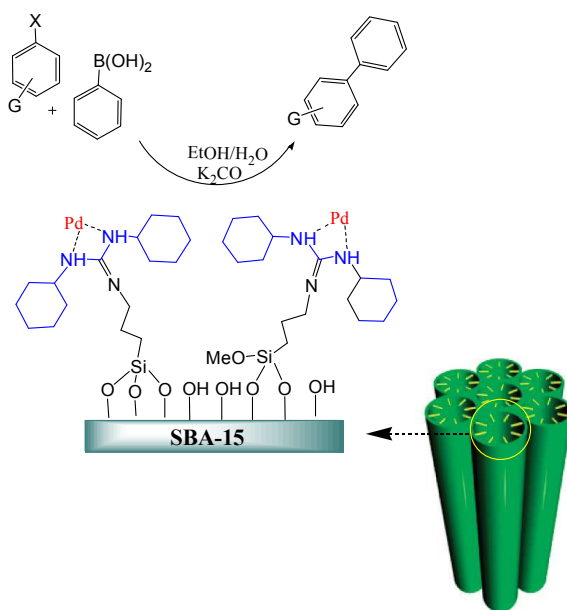
- 1 D. Rechavi and M. Lemaire, *Chem. Rev.* 2002, **102**, 3467.
- 2 Q. H. Fan, Y. M. Li, A.S.C. Chan, *Chem. Rev.* 2002, **102**, 3385.
- 3 A. Mandoli, S. Orlandi, D. Pini and P. Salvadori, *Chem. Commun.* 2003, **19**, 2466.
- 4 A. Choplin and F. Quignard, *Coord. Chem. Rev.* 1998, **178**, 1679.
- 5 D. R. Leonard and J. R. L. Smith, *J. Chem. Soc. Perkin Trans.* 1991, **2**, 25.
- 6 E. B. Cho, D. Kim, J. Gorka and M. Jaroniec, *J. Mater. Chem.* 2009, **19**, 2076.
- 7 A. Molnár, *Chem. Rev.* 2011, **111**, 2251.
- 8 H. Veisi, M. Hamelian and S. Hemmati, *J. Mol. Catal. A: Chem.* 2014, **395**, 25.
- 9 R. Ghorbani-Vaghei, S. Hemmati and H. Veisi, *J. Mol. Catal. A: Chem.* 2014, **393**, 240.
- 10 H. Veisi, D. Kordestani and A. R. Faraji, *J. Porous. Mater.* 2014, **21**, 141.
- 11 M. E. Davis, *Nature* 2002, **417**, 813.
- 12 A. Stein, *Adv. Mater.* 2003, **15**, 763.
- 13 H. Lee, S. I. Zones and M. E. Davis, *Nature* 2003, **425**, 385.
- 14 P. J. E. Harlick and A. Sayari, *Ind. Eng. Chem. Res.* 2007, **46**, 446.
- 15 Y. Mori and T. J. Pinnavaia, *Chem. Mater.* 2001, **13**, 2173.
- 16 Z. L. Lu, E. Lindner and H. A. Mayer, *Chem. Rev.* 2002, **102**, 3543.
- 17 A. P. Wight and M. E. Davis, *Chem. Rev.* 2002, **102**, 3589.
- 18 B. Karimi and D. Zareyee, *Org. Lett.* 2008, **10**, 3989.
- 19 M. A. Zolfigol, *Tetrahedron* 2001, **57**, 9509.
- 20 F. Hoffmann, M. Cornelius, J. Morell and M. Fröba, *Angew. Chem. Int. Ed.* 2006, **45**, 3216.
- 22 A. F. Schmidt and A. A. Kurokhitina, *Kinetics and Catalysis*, 2012, **53**, 714.
- 23 N. Jamwal, R. K. Sodhi, P. Gupta and S. Paul, *Int. J. Biol. Macromol.* 2011, **49**, 930.
- 24 Y. -Q. Tang, H. Lv, J. -M. Lu and L. -X. Shao, *J. Organomet. Chem.* 2011, 696, 3741.
- 25 Zhou, F. S. Liu, D. -S. Shen, Ch. Tan and L. -Y. Luo, *Inorg. Chem. Commun.* 2011, 14.

- 26 H. Veisi, R. Masti, D. Kordestani, M. Safaei and O. Sahin, *J. Mol. Catal. A: Chem.* 2014, **384**, 61.
- 27 H. Veisi, J. Gholami, H. Ueda, P. Mohammadi, M. Noroozi, *J. Mol. Catal. A: Chem.* 2015, **396**, 216.
- 28 (a) R. Ghorbani-Vaghei and H. Veisi, *J. braz. Chem Soc.*, 2010, **21**, 193; (b) H. Veisi, A. Sedrpoushan, P. Mohammadi, A. R. Faraji and Sami Sajjadifar, *RSC Advances.*, 2014, **4**, 25898; (c) H. Veisi, B. Maleki, F. Hosseini Eshbala, H. Veisi, R. Masti, S. Sedigh Ashrafi and M. Baghayeri, *RSC Adv.*, 2014, **4**, 30683; (d) R. Ghorbani-Vaghei, M. Chegini, H. Veisi and M. Karimi-Tabar, *Tetrahedron Lett.* **2009**, *50*, 1861. (e) H. Veisi, *Synthesis* 2009, 945; (f) H. Veisi *Synthesis* 2010, 2631; (g) H. Veisi, S. Hemmati, H. Veisi *J. Chin. Chem. Soc.* 2009, **56**, 240; (h) H. Veisi, *Tetrahedron Lett.* 2010, **51**, 2109; (g) A. Capan, H. Veisi, A. C. Goren, T. Ozturk, *Macromolecules* 2012, **45**, 8228.
- 29 L. Saikia, D. Srinivas and P. Ratnasamy, *Appl. Catal. A: Gen.* 2006, **309**, 144.
- 30 D. Zhang, Z. Liu, S. Han, C. Li, B. Lei, M. P. Stewart, J. M. Tour and C. Zhou, *Nano Lett.* 2004, **4**, 2151.
- 31 M. C. Militello and S. J. Simko, *Surf. Sci. Spectra*, 1994, **3**, 387.

Graphical Abstract

Palladium nanoparticles supported on 1,3-dicyclohexylguanidine functionalized Mesoporous silica SBA-15 as highly active and reusable catalyst for the Suzuki-Miyaura cross-coupling reaction

Hojat Veisi,* Abbas Amini Manesh, Neda Eivazi, Ali Reza Faraji



The synthesis and application of SBA-15/1,3-DCG/Pd as a novel heterogeneous and reusable nano catalyst in Suzuki reactions was described.